Removal of Malachite Green Dye from Aqueous Solutions by an Efficient Nanosized NiO Fabricated by a Facile Sol-Gel Autocombustion

Hesham H. El-Feky[1*], Reham N. Nassar[2], Alaa S. Amin[1*], Mostafa Y. Nassar[1*]

[1]*Department of Chemistry, Faculty of Science, Benha University, Benha 13815, Egypt.*
[2]*Central Laboratory for Environmental Quality Monitoring (CLEQM), National Water Research Center (NWRC), Cairo, Egypt.*

Authors' contributions

This work was carried out in collaboration among all authors. All authors read and approved the final manuscript.

Original Research Article

ABSTRACT

Nickel oxide nanostructures were synthesized via a sol-gel combustion method using glucose, glycine and tartaric acid fuels. The effect of the fuel type on the formed nanostructures was studied. The as-prepared products were characterized by means of FE-SEM, HR-TEM, XRD, and FT-IR analyses. The results exhibited that the used fuels gave NiO products with different morphologies, and the glucose fuel produced pure NiO nanoparticles with the smallest crystallite size (ca. 8.2 nm). The adsorption properties of the NiO products for the removal of malachite green dye (MG) was examined. Using a batch method, various parameters affecting the adsorption properties were studied. The results revealed that NiO nanostructure generated from the glucose fuel had the highest adsorption capacity

_____

Corresponding author: E-mail: hesham.elfeky@fsc.bu.edu.eg, asamin2005@hotmail.com, m_y_nassar@yahoo.com;

1. INTRODUCTION

The emergence of nanotechnology has provided an extensive research in recent years by intersecting with various other branches of science and forming impact on all forms of life. Nanoparticles are a class of materials with properties distinctively different from their bulk and molecular counterparts [1]. Nano particles and Nano materials are finding an ever-increasing range of applications [2]. Traditionally, nanoparticles have been synthesized by physicochemical methods. However, these methods have disadvantages, including the use of costly and toxic reagents and the need for aggressive physical treatments (elevated pressure and irradiation, pH, and temperature [3]. Numerous chemical techniques for the preparation of nanoparticles have been studied. Among those methods, sol–gel auto combustion technique is the most popular technique [4,5]. The principle and the nomenclature of combustion synthesis as it is a method of synthesizing high-temperature materials of inorganic compounds. It is also called self-propagation high-temperature synthesis, or SHS for short. The principle is to use the self-heating and self-conduction effects of high chemical reaction heat between reactants to synthesize materials [6,7].

Transition metal oxides (TMOs) have shown noticeable properties such as structural flexibility, optical, electrical and magnetic properties because of their surface properties, electronic structure and defects [8]. Among other TMOs, the NiO particles show many unique magnetic, optical, electronic, and chemical properties, so they have shown great potential for application in various electrochemical systems as cathode material, solid oxide fuel cells (SOFC), dye-sensitized solar cells, semi-conductors, p-type transparent conducting films, catalysis, anti-ferromagnetic layers, gas sensors, etc [9,10]. Nickel oxide (NiO), has a wide band gap [11] and varied applications [12]. They include catalysis [11], lithium ion batteries [13], smart windows [11], antiferromagneticfilm [14] photocatalysis [15], antimicrobialactivity [11], thermal conductivity [16] and field emission studies [17]. Recent studies of nickel oxide nanoparticles (NiO NPs) prepared by a cost-effective and eco-friendly method have been used to evaluate its antimicrobial activity [18].

Metal oxides (MO) are synthesized by different methods as spray pyrolysis, sputtering, electrodeposition, thermal decomposition, sol–gel techniques, chemical bath deposition, co-precipitation, hydrothermal method, etc [19-24]. As previously reported work, the nanoparticles of NiO synthesized through a combustion technique, has significantly overstepped all other techniques like, hydrothermal, sol gel, chemical precipitation, green synthesis and caclined hydrothermal method, therefore, the purpose of this study is to develop anovel method for the production of NiO nanoparticles by combustion process (CS) [25-28].

Dyes are widely utilized in large industries such as paper, food, cosmetics, plastics and textile [29]. They represent a contaminant of concern for water resources, due to their poor biodegradability and also because of their high diffusion in aquatic environment [30]. Malachite green (MG), tri-phenyl methane dye, has been widely used for the dyeing of leather, wool and silk as well as in distilleries [31]. However, MG is very dangerous and highly cytotoxic to mammalian cells, and also acts as a liver tumor-enhancing agent [32]. Therefore, there is considerable need to treat these effluents into receiving waters to prevent environmental pollution in the aquatic systems. Different techniques have been investigated to eliminate color from dye house effluents, varying in effectiveness, economic cost, and environmental impact (of the treatment process itself). Among all of the treatments proposed, the adsorption of dye molecules onto a substrate (adsorbent) can be a very effective, low-cost method of color removal [33,34].

Herein, we have developed a facile, inexpensive approach for NiO nanoparticles via an auto-combustion method employing nickel nitrate as an oxidant and glucose fuel as a reductant. The synthesized nanostructures were characterized by X-ray diffraction (XRD), Fourier transforms infrared spectroscopy (FTIR), field-emission scanning electron microscope (FE-SEM), and high-resolution transmission electron microscope (HR-TEM). Indeed, in this report, we wish to study the performance and capacity of adsorption of malachite green (MG) from water via synthesized NiO nanoparticles. Besides, the adsorption isotherm and kinetic of MG onto the nanocomposite was investigated as well.

2. MATERIALS AND METHODS

2.1 Chemicals and Reagents

All materials and reagents in the current study were used as received without further purification

since they were of analytical grade. Nickel Nitrate (Hexahydrate) [Ni (NO$_3$) $_2$. 6H$_2$O, M.WT.(290.80 g/mole)] (Merk). Anhydrous glucose [C$_6$H$_{12}$O$_6$, M.WT.(180 g/mole)], glycine [C$_2$H$_5$NO$_2$, M.WT.(75 g/mole)] and Tartaric acid [C$_4$H$_6$O$_6$, M.WT.(150 g/mole)] (Elnasr for chemicals, Egypt). The prepared NiO nanostructures were characterized by X-ray diffraction (XRD), Fourier transforms infrared spectroscopy (FTIR), field-emission scanning electron microscope (FE-SEM), and high-resolution transmission electron microscope (HR-TEM).

2.2 Preparation of NiO Nanoparticles

NiO nanoparticles were prepared by using hexa-hydrated nickel nitrate [Ni(NO$_3$)$_3$.6H$_2$O] as an oxidant precursor and the fuels were used as reductant precursors. The produced NiO samples by using three different fuels: glucose, glycine and tartaric acid are referred by A, B and C, respectively. The stoichiometric compositions of the redox mixtures for the combustion have been calculated based on the total oxidising {O} and reducing {F} valencies of the oxidizer and fuel so that the equivalence ratio, ϕ_c is unity (i.e. ϕ_c =(O/F)=1), and consequently the energy released by the combustion is maximum for each reaction [35].

In a typical synthesis process: 20 ml of Ni(NO$_3$)$_3$.6H$_2$O (8 g, 0.02 mol) was mixed with an aqueous hot solution (50 ml), containing glucose (1.77g, 0.01mol) and the reaction was heated at 80°C, and allowed to stir for 15 min. The produced solution was gelled while heating at 120°C. The formed gel was ignited on a hot plate at 350°C give a dry and black mass which was then calcined in an electric furnace at 600°C for 2 hrs, naming (A$_{600}$). The produced nickel oxide samples (B$_{600}$ and C$_{600}$) were prepared by applying similar conditions [36].

3. RESULTS AND DISCUSSION

3.1 Fuel Effect

A modified sol–gel auto combustion method was used in this work to synthesize NiO nanoparticles based on different kinds of fuels such as : glucose, glycine and tartaric acid. The used organic fuels in this investigation played here as they serve as fuels, in the combustion reaction, oxidized by the nickel nitrates, to produce NiO nanoparticles. The proposed equations 1–3 for the combustion reactions (Scheme 2S) revealed that the molar ratios of Ni^{2+}: glucose, Ni^{2+}: glycine, and Ni^{2+}: tartaric acid, are 2.7:1, 1:1.11, and 1:1, respectively, corresponds to the situation of an "equivalent stoichiometric ratio". In this combustion process, the reaction between the oxidizers (nickel salt) and the fuel is an exothermic reaction which implies that the oxygen content of salt nitrates can be completely reacted to oxidize/consume the used fuel exactly results in enough heat for producing the nanomaterials of interest [37]. In addition to producing of the nano-sized NiO product, these reactions give off CO$_2$, H$_2$O, and N$_2$ gases directly from the reaction between fuel and oxidizer without any need for supplying oxygen from outside except in case of glucose. The products were characterized by means of XRD, FT-IR, UV–Vis spectra, FE-SEM and HR-TEM.

$$2.7Ni(NO_3)_2.6H_2O_{aq} + C_6H_{12}O_{6_{aq}} + 1.35\ O2 \rightarrow 2.7NiO_s + 16.2H_2O_g + 6CO_{2_g} + 2.7N_{2_g} \qquad \text{Eq(1)}$$

$$Ni(NO_3)_2.6H_2O_{aq} + 1.11C_2H_5NO_{2_{aq}} \rightarrow NiO_s + 8.77H_2O_g + 2.22CO_{2_g} + 1.55N_{2_g}\ \text{Eq(2)}$$

$$Ni(NO_3)_2.6H_2O_{aq} + C_4H_6O_{6_{aq}} \rightarrow NiO_s + 9H_2O_g + 4CO_{2_g} + N_{2_g} \qquad \text{Eq(3)}$$
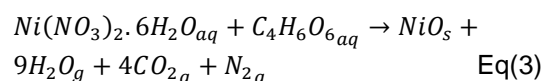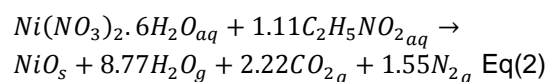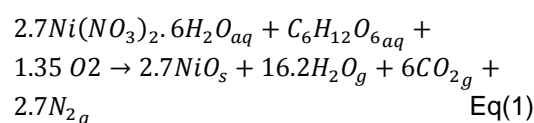
3.2 X-Ray Diffraction (XRD) study NiO Nanoparticles

In case of the products (B and C) except (A) formed by 600 °C, the sites and intensity of the diffraction peaks are consistent with the standard pattern for JCPDS card No. (00-011-4459) Nickel oxide (Fig. 1). XRD patterns of NiO samples (B and C) except (A) calcined at 600°C for 2 hrs are almost identical showing broad peaks, indicating small crystalline size of the particles and the fine nature [38].

The crystallite size (D, nm) of the NiO nanoparticles can be evaluated [39,40]:

$$\text{D} = 0.9\lambda\ /\ \beta\cos\theta_B\ (2)\ \text{Eq(4)}$$

Where β is the full-width at half-maximum (FWHM) value of XRD diffraction lines, the wavelength λ=0.154056 nm and Θ is the half diffraction angle of 2Θ. The lattice constants are equal (a = b =4.7588 and c = 12.9920 A°) ensure the formation of a Rhombohedral structure. The average particle size was found to be 28.2 nm and 40.3 nm for B and C samples, consequently.

For sample (A) formed by glucose at 600°C, the sites and intensity of the diffraction peaks are consistent with the standard pattern for JCPDS card No. (00-004-0835) Nickel oxide (Fig. 1). The lattice constants are equal (a = b = c = 4.1769 A°) ensure the formation of a cubic structure. The diffraction peaks at 37.28°, 43.298°, 62.917°, 75.445°, 79.393° and 95.083° are indexed to the following planes (1 1 1), (2 0 0), (2 2 0), (3 1 1), (2 2 2) and (4 0 0) of the cubic unit cell. Its average particle size was found to be 8.2, consequently A_{600} has the best crystal size.

3.3 FT-IR study

The infrared spectra of the as-prepared NiO nanoparticles annealed at 600°C are shown in Fig. 2, it seems that the three spectra are almost identical. In Fig. 2, the NiO samples exhibited characteristic frequency in the region of 400−684 cm^{-1} correspond to the existence of NiO. In the IR spectra, the NiO sample exhibited characteristic frequency at 404–512 cm^{-1} ,406-439 cm^{-1} and 401-491 cm^{-1} respectively are associated with the special vibration of Nickel oxide, and indicating the formation of NiO samples. However, the IR spectra show broad vibration band at 3423cm^{-1}, 2924 cm^{-1}, and 2855 cm^{-1} respectively are associated with the OH stretching vibrations of water molecules (physical adsorbed molecular water), while those at 1656 cm^{-1}, 1628 cm^{-1} and 1608 cm^{-1} are associated with their bending mode. The band at 1383 cm^{-1},1346 cm^{-1} and 1191cm^{-1} respectively could be ascribed to stretching vibration of CO_2, the band 437cm^{-1} characteristic absorption peak of CO_3^{2-} New bands were observed within a range from 437 $cm^{-1}$to 550 cm^{-1} that were identified as the characteristic bands of Ni-O stretching. The peak at 481 cm^{-1} is attributed by bending vibrations of metal oxide (Ni-O-Ni) nanoparticles [41,42].

3.4 Morphology Study of NiO Nanoparticles

3.4.1 Field emission scanning electron microscopy (FE-SEM) of NiO nanoparticles

Morphologies of the as-prepared NiO sample calcined at 600°C (A_{600}) was investigated by using field emission scanning electron microscopy (FE-SEM) and presented in Fig. 3. From SEM micrographs of A_{600} powders, rough surfaces and many visible mesoporous are observable in the micrographs with a wide distribution [43].

3.4.2 High-resolution transmission electron microscopy (HR-TEM) of NiO nanoparticles

Morphological and Structural characterization of green synthesis NiO NPs (A_{600}), were analyzed by HR-TEM. As shown in Fig. 4 the product A_{600} is composed of dispersed cubic particles with an average diameter of 9.3 nm which is compatible with the crystalline size calculated from the XRD studies [43].
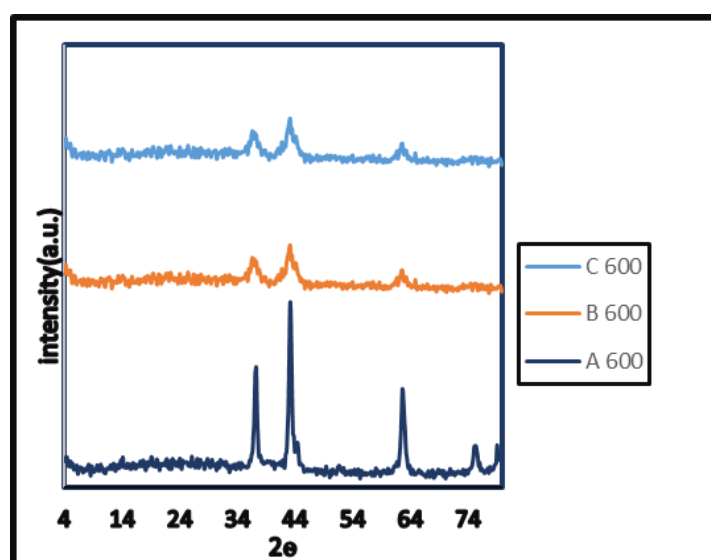
Fig. 1. XRD patterns of NiO samples (A, B and C) calcined at 600°C prepared using glucose, glycine and tartaric fuels, respectively
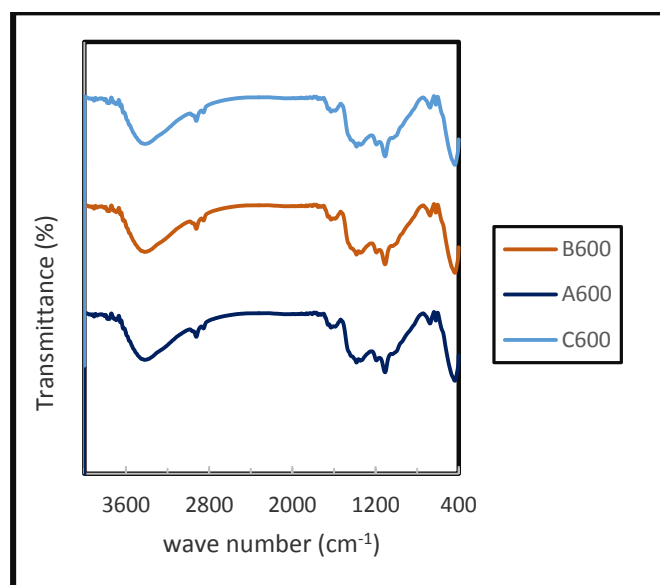
Fig. 2. FT-IR spectra of NiO samples (A, B and C) calcined at 600°C prepared using Glucose, glycine and tartaric fuels, respectively
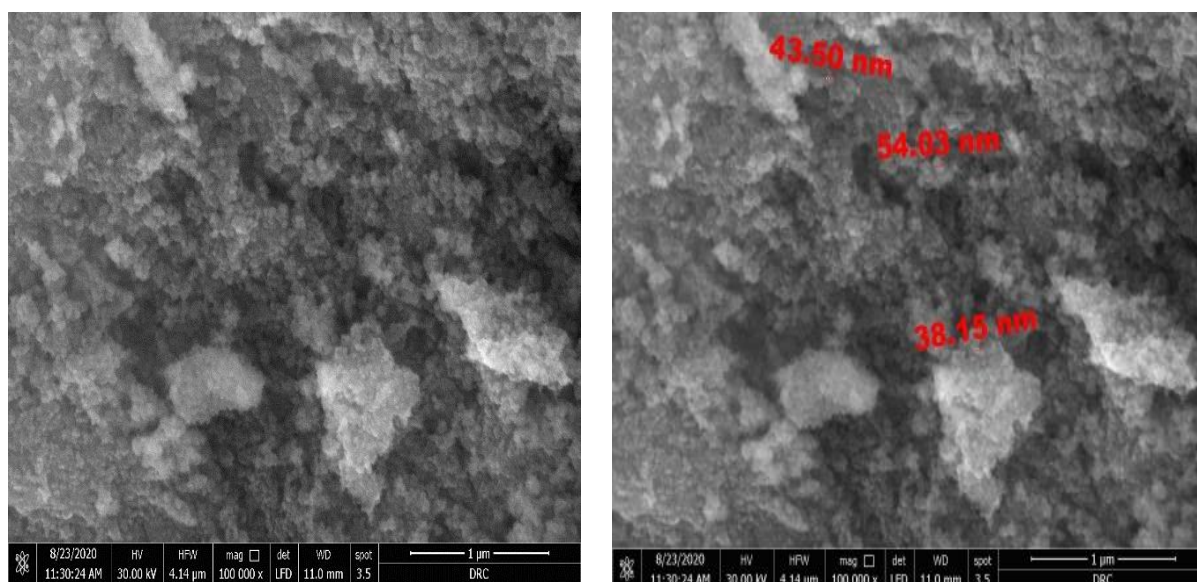
Fig. 3. FE-SEM images of NiO product A$_{600}$ calcined at 600°C

4. ADSORPTION STUDIES

4.1 Characteristic Adsorption Capacity of NiO (A$_{600}$) Sample

One of the most characteristics applications to test the ability of nanostructures for dye removal is the adsorption capacity. Many factors affecting the removal of MG from water such as pH, dosage level of nanoparticles, temperature, contact time and the initial concentration of MG were studied.

4.2 Factors Affect the Adsorption Process

4.2.1 Effect of pH

The most important parameter influencing adsorption efficiency is pH of the adsorption medium. The initial concentration of MG, NiO dose, volume of MG dye and the stirring rate were set at 50 ppm, 0.05 g, 50 mL and 400 rpm, respectively at 298 K for 1 h. The effect of initial pH of the solution on the MG dye and removal

efficiency onto NiO powder was assessed over a wide pH range from 2.6 to 9.47 with a stirring time of 1 hr. As shown in Fig. 5 at lower pH = 2.6, the smallest percent (87.7 %) of MG dye was adsorbed on the surface of the adsorbent, while the highest percent of removal was obtained at pH = 8, 96.97% of MG dye was adsorbed. This means that the alkaline medium is favorable for the adsorption process of MG dye. The number of negatively charged sites on the NiO surface enhance and a significantly strong electrostatic attraction appears between adsorbent and cationic MG molecule, while the reveres occur at lower pH 2.6 [44].

4.2.2 Effect of contact time

The time dependent behavior of MG dye adsorption was examined by varying the contact time between adsorbate and adsorbent in the range of 30–150 min. The initial concentration of MG, NiO dose, volume of MG dye, pH and the stirring rate were set at 50 ppm, 0.05 g, 50 mL, 8 and 400 rpm, respectively at 298 K for 1 h. Fig. 6 shows that the removal percent for MG dye by the adsorbent is rapid and thereafter it proceeds at a slower rate and finally attains saturation. The rate of removal of the adsorbate is higher in the beginning due to the large surface area of the
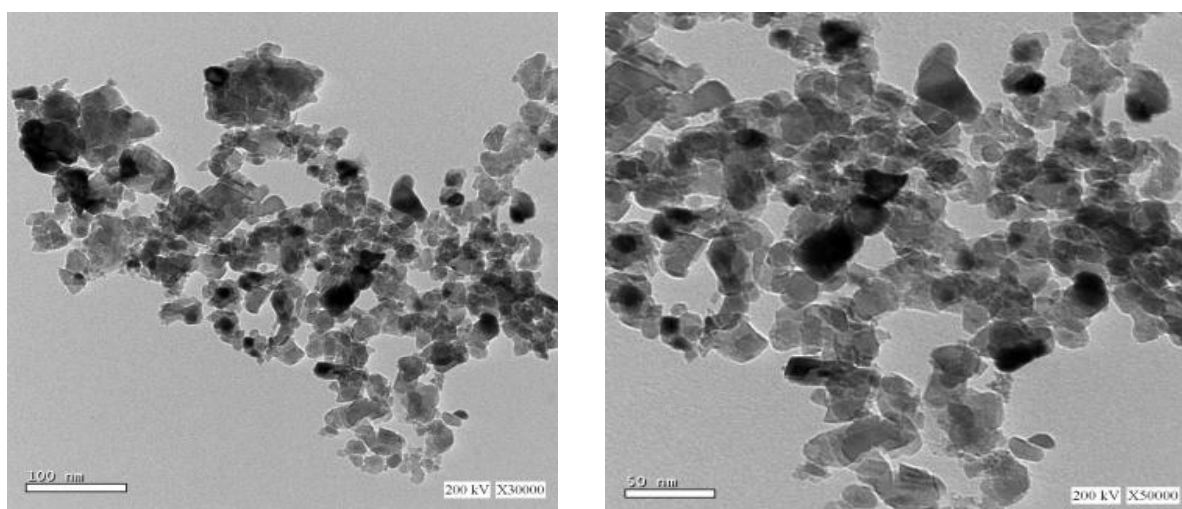
Fig. 4. TEM image of of NiO product A_{600} calcined at 600°C
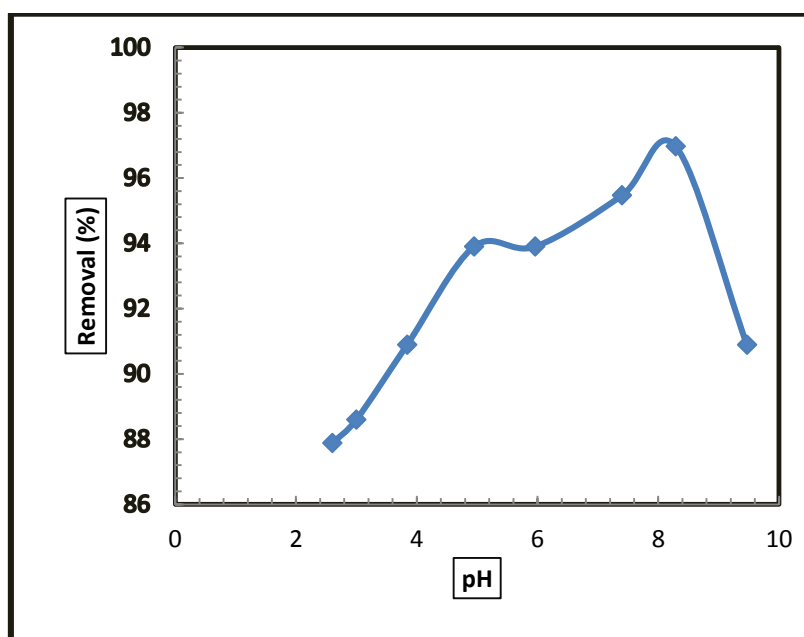
Fig. 5. Effect of pH on MG removal percent using NiO (A_{600})

adsorbent available for the adsorption observed because there are few active sites on the surface of sorbent. The optimum time duration required for MG dye removal (92.16%) was 105 min.

4.2.3 Effect of temperature

The adsorption studies were carried out at three different temperatures 25, 35 and 45 °C. Results in Fig.7 showed that the adsorption efficiency increased with increasing temperature, which shows that the removal of MG dye is favored at high temperatures and the removal process is endothermic process. The increase in the rate of adsorption with the increase in temperature may be attributed to the high mobility of dye molecules, negatively charged, at high temperatures results in increasing the tendency or velocity of dye molecules towards the positive charge at NiO surface positively charged.

4.2.4 Effect of initial dye concentration

One of the most important variables that can affect the adsorption process initial heavy metal concentration. The effect of initial concentration of MG between (50-180) mg/L was studied on its adsorption onto NiO under previously determined optimum conditions and at room temperature. The results, in terms of removal efficiency versus initial concentration (mg/L), of MG are indicated in Fig. 8. It can be seen from the results that the percentage removal decreases with the increase in initial concentration, where it is seen that the adsorption of MG decreased gradually from 97.7% to 62%. Sufficient adsorption sites are

available at lower initial concentrations, but at higher concentrations dye particles are greater than adsorption sites. Thus, it can be said that removal of mercury is concentration dependent using NiO as previously reported [45].

4.2.5 Effect of adsorbent dose

The effect of adsorbent dose on the MG dye removal was demonstrated in Fig. 9. The effect of adsorbent quantity of removal of MG is presented in Fig. 9. The removal of MG was investigated by adding various amount of adsorbent in the range of 0.05-0.2 g powder into a flask containing 50 ml of 50 ppm MG solution at pH= 8. It shows that as the adsorbent dose was increased from 1 to 1 g/L, the removal percent increased from 88.2% to 99.8% for NiO. This may be due to the availability of surface activities resulting from the increased dose and agglomeration of the adsorbent.

4.2.6 Effect of ionic strength

The influence of ionic strength on the adsorption of MG onto NiO was investigated using KCl salt of doses ranging from 0.05 g/L to 0.45 g/L, at constant dye concentration of 50 mg/L. The effect of ionic strength on the adsorption ability was demonstrated in Fig.10. It was observed that as the ionic strength (dose of KCl) increases, the adsorption efficiency of NiO decreases, this is due to the cations of salt competing with the dye species towards the surface of NiO. The salt ions also screen the surface of the adsorbent.
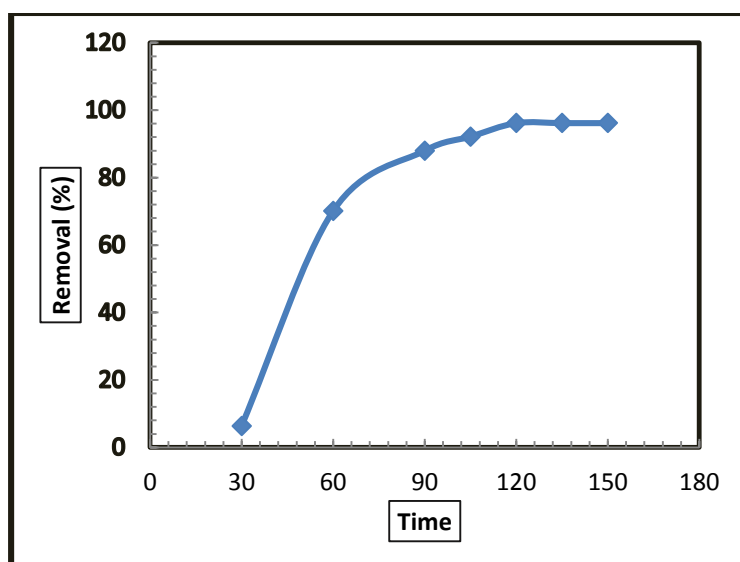
Fig. 6. Effect of contact time on MG removal percent using NiO (A_{600})
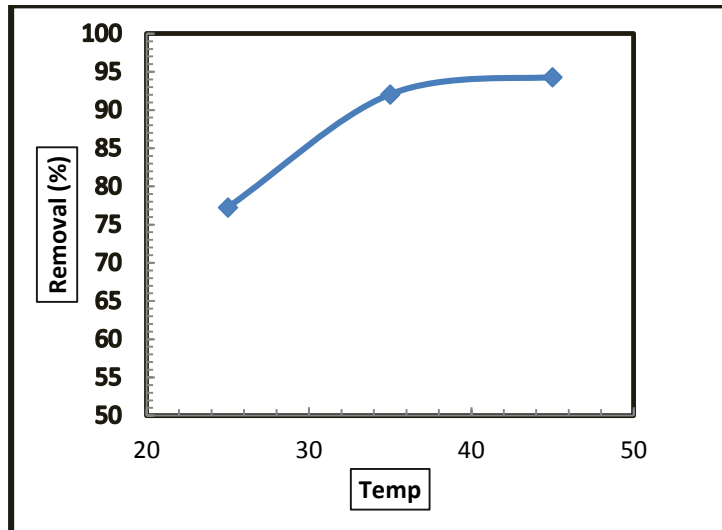
Fig. 7. Effect of temperature on MG removal percent using NiO (A$_{600}$)
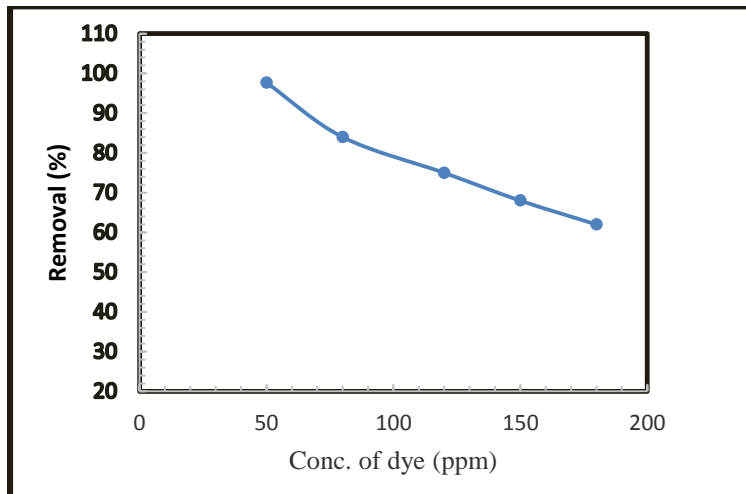
Fig. 8. Effect of initial concentration of MG removal percent using NiO (A$_{600}$)
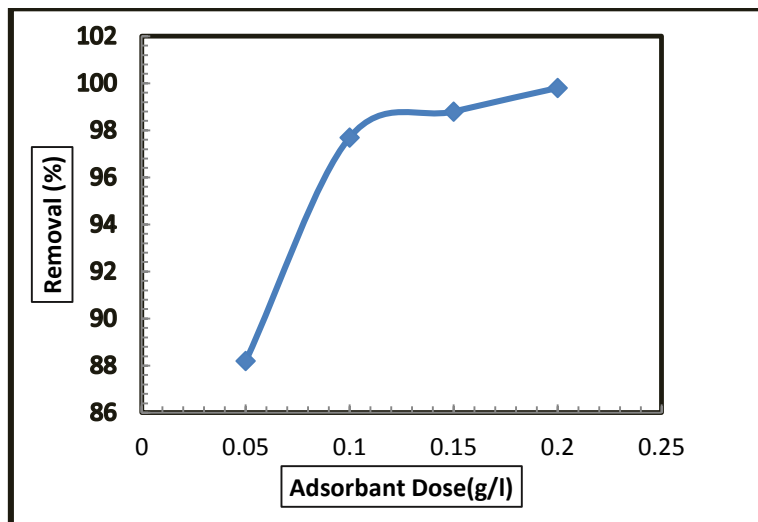
Fig. 9. Effect of adsorbent dose on MG removal percent using NiO (A$_{600}$)
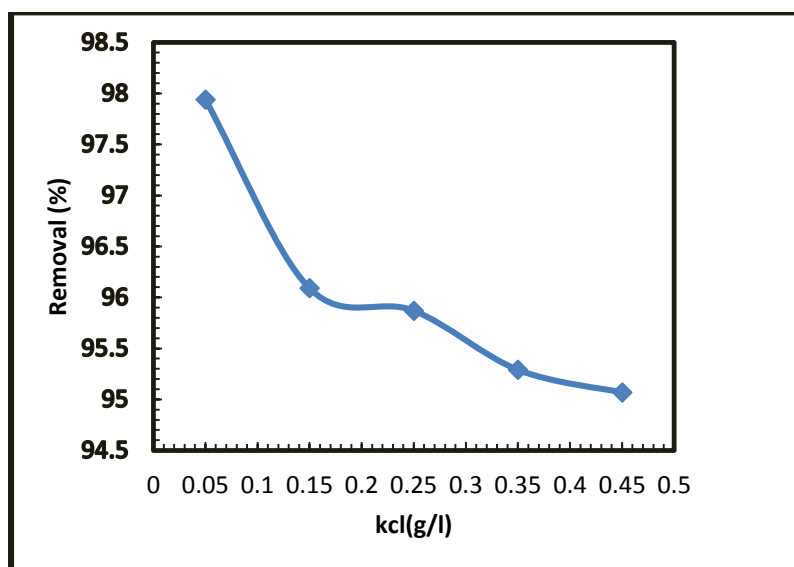
Fig. 10. Effect of KCl concentration on dye removal percent of MG using A$_{600}$

5. CONCLUSION

In summary, a facile and green treatment of Ni salts produced pure NiO nanoparticles using auto combustion method under optimized experimental conditions. NiO nanostructures have been prepared by using a facile, inexpensive, economical auto-combustion approach. In this method Nickel nitrate and different fuels were used as an oxidant and a reductant, respectively. Glucose fuel gave pure cubic NiO product with the smallest crystallite size (~8.2 nm). The as-prepared NiO nanoparticles displayed good adsorption capacity for malachite green (MG) dye [46].

COMPETING INTERESTS

Authors have declared that no competing interests exist.

REFERENCES

1. Pachon LD, Rothenberg GJAOC. Transition- metal nanoparticles: Synthesis, stability and the leaching. 2008;22(6):288-299.
2. Biswas P, Wu CYJJOTA, Association WM. Nanoparticles and the environment. 2005;55(6):708-746.
3. Kon K, et al. Fungi as an efficient mycosystem for the synthesis of metal nanoparticles: Progress and Key Aspects of Research; 2015.
4. Novitskaya E, et al. A review of solution combustion synthesis: An analysis of parameters Controlling Powder Characteristics. 2021;66(3):188-214.
5. Pei L, et al. Preparation of low temperature cure polybenzoxazine coating with enhanced thermal stability and Mechanical Properties by Combustion Synthesis Approach. 2021;220:123573.
6. Wu H, et al. One- pot solution combustion synthesis of crystalline and amorphous molybdenum trioxide as anode for Lithium- Ion Battery. 2021;104(2):1102-1109.
7. Kermani F, et al. Solution combustion synthesis (SCS) of theranostic ions doped biphasic calcium phosphates; kinetic of ions release in simulated body fluid (SBF) and Reactive Oxygen Species (ROS) Generation. 2021;118:111533.
8. Sonal S, Mishra BKJCEJ. A comprehensive review on the synthesis and performance of different zirconium-based adsorbents for the removal of various water contaminants. 2021;130509.
9. Ahmad J, et al. Strontium-Doped Nickel Oxide Nanoparticles: Synthesis, Characterization, and Cytotoxicity Study in Human Lung Cancer A549 Cells. 2021;1-10.
10. Gautam C, et al. Syntheses, Characterization and Oxygen Evolution Reaction (OER) Electrocatalytic Properties of M (II) based Bromo-Salophen Complexes. 2021;130928.
11. Ramasami AK, Reddy M, Balakrishna GR. Combustion synthesis and characterization of NiO nanoparticles. Materials Science in

Semiconductor Processing. 2015;40:94-202.

12. Anandan K, Rajendran V. Structural, optical and magnetic properties of well-dispersed NiO nanoparticles synthesized by CTAB assisted solvothermal process. Nanosci. Nanotechnol. Int. J. 2012;2(4):24-29.

13. Sun W, et al. Ultrathin nickel oxide nanosheets for enhanced sodium and lithium storage. Journal of Power Sources. 2015;274:755-761.

14. Loudon J. Antiferromagnetism in NiO observed by transmission electron diffraction. Physical Review Letters. 2012;109(26):267204.

15. Nitin C, et al. Photocatalytic degradation of safranine O in the presence of nickel oxide. International Journal of Research in Chemistry and Environment (IJRCE). 2011;1(1):66-70.

16. Sahoo P, et al. Thermal Conductivity of Nickel Oxide Nanoparticles Synthesized by Combustion Method. MRS Online Proceedings Library (OPL). 2010;1256.

17. Varghese B, et al. Fabrication of NiO nanowall electrodes for high performance lithium ion battery. Chemistry of Materials. 2008;20(10):3360-3367.

18. Rakshit S, et al. Controlled synthesis of spin glass nickel oxide nanoparticles and evaluation of their potential antimicrobial activity: A cost effective and eco friendly approach. RSC Advances. 2013;3(42):19348-19356.

19. Abbas H, et al. Photocatalytic activity and two-magnon behavior in nickel oxide nanoparticles with different silica concentration. 2019;125(14):144305.

20. Carney C, et al., Rapid nickel oxalate thermal decomposition for producing fine porous nickel metal powders: Part 3: Mechanism. 2006;431(1-2):26-40.

21. Carney CS, et al. Rapid nickel oxalate thermal decomposition for producing fine nickel metal powders: Part 2: Global Kinetics. 2006;431(1-2):13-25.

22. Dong L, Chu Y, Sun WJCAEJ.. Controllable synthesis of nickel hydroxide and porous nickel oxide nanostructures with different morphologies. 2008;14(16):5064-5072.

23. Uddin J, et al. Influence of Ni doping on the morphological, structural, optical and electrical properties of CuO thin films deposited via a spray pyrolysis. 2021;119:111388.

24. Wang WN, et al. Nickel and nickel oxide nanoparticles prepared from nickel nitrate hexahydrate by a low pressure spray pyrolysis. 2004;111(1):69-76.

25. Park J, et al. Monodisperse nanoparticles of Ni and NiO: Synthesis, characterization, self-assembled superlattices, and catalytic applications in the Suzuki coupling reaction. 2005;17(4):429-434.

26. Bonomo MJJoNR. Synthesis and characterization of NiO nanostructures: A review. 2018;20(8):1-26.

27. Alagiri M, Ponnusamy S, Muthamizhchelvan CJJOMSMIE. Synthesis and characterization of NiO nanoparticles by sol–gel method. 2012;23(3):728-732.

28. Nassar MY, et al. Synthesis, characterization, and biological activity of some novel Schiff bases and their Co (II) and Ni (II) complexes: A new route for Co3O4 and NiO nanoparticles for photocatalytic degradation of methylene blue dye. 2017;1143:462-471.

29. Mittal A, et al., Adsorption studies on the removal of coloring agent phenol red from wastewater using waste materials as adsorbents. 2009;337(2):345-354.

30. Zamouche M, Arris S, LeHocine MBJIJOHE. Removal of Rhodamine B from water by cedar cone: Effect of calcinations and chemical activation. 2014;39(3):1523-1531.

31. Zhang J, et al. Adsorption of malachite green from aqueous solution onto carbon prepared from Arundo Donax Root. 2008;150(3):774-782.

32. Bekçi Z, Seki Y, Cavas LJJOHM. Removal of malachite green by using an invasive marine alga Caulerpa racemosa var. Cylindracea. 2009;161(2-3):1454-1460.

33. San Miguel G, et al. A practical review of the performance of organic and inorganic adsorbents for the treatment of contaminated waters. 2006;81(10):1685-1696.

34. Nassar MY, et al. MgO nanostructure via a sol-gel combustion synthesis method using different fuels: An efficient nano-adsorbent for the removal of some anionic textile dyes. 2017;225:730-740.

35. Ramasami AK, Reddy M, Balakrishna GRJMSISP. Combustion synthesis and characterization of NiO nanoparticles. 2015;40:194-202.

36. Zhang G, Shen X, Yang Y. Facile synthesis of monodisperse porous ZnO

spheres by a soluble starch-assisted method and their photocatalytic activity. The Journal of Physical Chemistry C. 2011;115(15):7145-7152.

37. Nassar MY, et al. A novel synthetic route for magnesium aluminate (MgAl2O4) nanoparticles using sol–gel auto combustion method and their photocatalytic properties. 2014;131:329-334.

38. Yu J, et al. Synthesis of alumina nanosheets via supercritical fluid technology with high uranyl adsorptive capacity. New Journal of Chemistry. 2013;37(2):366-372.

39. Holzwarth U, Gibson N. The Scherrer equation versus the'Debye-Scherrer equation'. Nature Nanotechnology. 2011;6(9):534-534.

40. Bedi RK, Singh I. Room-temperature ammonia sensor based on cationic surfactant-assisted nanocrystalline CuO. ACS Applied Materials & Interfaces. 2010;2(5):1361-1368.

41. Khalaji AD, Das D. Synthesis and characterizations of NiO nanoparticles via solid-state thermal decomposition of nickel (II) Schiff base complexes. International Nano Letters. 2014l4(3):1-5.

42. George G, Anandhan S. Electrospun nickel oxide nanofiber webs for thermistor applications. International Journal of Plastics Technology. 2014;18(3):374-382.

43. Boudiaf M, et al. Green synthesis of NiO nanoparticles using Nigella sativa extract and their enhanced electro-catalytic activity for the 4-nitrophenol degradation. Journal of Physics and Chemistry of Solids. 2021;153:110020.

44. Ge Y, et al. Heavy metal ions retention by bi-functionalized lignin: Synthesis, applications, and adsorption mechanisms. Journal of Industrial and Engineering Chemistry. 2014;20(6):4429-4436.

45. Raval NP, Shah PU, Shah NKJAWS. Malachite green a cationic dye and its removal from aqueous solution by Adsorption. 2017;7(7):3407-3445.

46. Mayedwa N, et al. Green synthesis of nickel oxide, palladium and palladium oxide synthesized via Aspalathus linearis natural extracts: Physical properties & mechanism of formation. Applied Surface Science. 2018;446:266-272.

Peer-review history:
The peer review history for this paper can be accessed here:
https://www.sdiarticle4.com/review-history/73529